

Critical temperature of superconducting bilayers: Theory and experiment

G. Brammertz^{a)}

Science Payloads Technology Division, Research and Scientific Support Department, European Space Agency, ESTEC, Keplerlaan 1, 2200 AG Noordwijk, The Netherlands

A. A. Golubov

Department of Applied Physics, University of Twente, P.O. Box 217, 7500 AE Enschede, The Netherlands

P. Verhoeve, R. den Hartog, and A. Peacock

Science Payloads Technology Division, Research and Scientific Support Department, European Space Agency, ESTEC, Keplerlaan 1, 2200 AG Noordwijk, The Netherlands

H. Rogalla

Department of Applied Physics, University of Twente, P.O. Box 217, 7500 AE Enschede, The Netherlands

(Received 18 December 2001; accepted for publication 26 February 2002)

A generalized model for the critical temperature T_C of superconducting bilayers is presented, which is valid with no restrictions to film thicknesses, T_C of the layers, and interface resistivity. The model is verified experimentally on a series of Nb–Al and Ta–Al bilayers with Nb, Ta layer thicknesses of 100 nm and Al layer thicknesses ranging from 5 to 200 nm. Excellent agreement between theory and experiment was found for the energy gap and the T_C of bilayers. The results are important for designing practical superconducting devices. © 2002 American Institute of Physics.
[DOI: 10.1063/1.1470712]

There is presently a growing interest in the development of superconducting bilayers S_1 – S_2 for a number of practical applications, like tunnel junctions for x-ray detection,^{1–4} transition edge sensors,^{1,2,5} and Josephson junctions.⁶ When designing such devices, it is often necessary to adjust and predict the bilayer transition temperature T_C . Although the proximity effect theory has been extensively developed during the last decade, there was certainly a lack of practically oriented studies of T_C in bilayers. In early work on the proximity effect,^{7–10} the approximate methods for the determination of T_C were developed. However, the boundary conditions used do not follow from the microscopic theory of superconductivity, (see also the review in Ref. 11). More recently, the microscopic theory in the dirty limit based on the Usadel equations¹² was used to calculate T_C of *bi*- and multilayered systems, but only limiting cases were studied: high transparency of S_1 – S_2 interface,^{13,14} finite transparency of S_1 – S_2 interface but thin or thick S_2 layers, and zero T_{CS_2} ,^{15,16} or the limit of very thin S_1 and S_2 layers.^{17,18}

In this letter, the generalized model for T_C of superconducting bilayers is presented without restriction to the S_1 and S_2 layer thicknesses, $T_{CS_1S_2}$ values, material parameters, and resistivity of the S_1 – S_2 interface. The model is verified experimentally on a series of Nb–Al and Ta–Al bilayers.

We consider a bilayer structure consisting of S_1 and S_2 layers of thickness d_{S_1} and d_{S_2} , respectively. Finite transparency of the S_1 – S_2 boundary can result either from a difference in Fermi velocities of the materials or from the existence of a potential barrier at the interface. In general, the S_2 material is also superconducting with a transition temperature $T_{CS_2} < T_{CS_1}$. Our assumption is that the materials are either in the dirty limit or in the clean limit with, in that case

only, the additional condition of diffusive scattering at the film interfaces. Under these assumptions and in the vicinity of the transition temperature T_C , the proximity effect is described by the linearized set of Usadel equations¹² in material $i = 1, 2$:

$$\Phi_{S_i} = \Delta_{S_i} + \frac{D_{S_i}}{2\omega_n G_{S_i}} [G_{S_i}^2 \Phi'_{S_i}], \quad (1)$$

$$\Delta_{S_i} \ln \frac{T_C}{T_{CS_i}} + 2\pi T_C \sum_{\omega_n > 0} \frac{(\Delta_{S_i} - \Phi_{S_i} G_{S_i})}{\omega_n} = 0, \quad (2)$$

Φ_{S_i} and $G_{S_i} = \omega_n / (\omega_n^2 + \Phi_{S_i}^2)^{1/2}$ are the normal and anomalous Green's functions, Δ_{S_i} is the order parameter, and D_{S_i} is the diffusion coefficient in the S_1 and S_2 layers, respectively. $\omega_n = \pi T(2n + 1)$ is the Matsubara frequency. Equations (1) and (2) are supplemented with the boundary conditions at the free surfaces, $\Phi'_{S_1} = 0$ at $x = d_{S_1}$, $\Phi'_{S_2} = 0$ at $x = -d_{S_2}$, and at the S_1 – S_2 interface¹⁹ ($x = 0$):

$$D_{S_1}^{1/2} G_{S_1}^2 \Phi'_{S_1} = \gamma \Delta_{S_2}^{1/2} G_{S_2}^2 \Phi'_{S_2}, \quad (3)$$

and

$$\gamma_{BN} \xi_{S_2}^* G_{S_2}^2 \Phi'_{S_2} = G_{S_1} (\Phi_{S_1} - \Phi_{S_2}), \quad (4)$$

where $\xi_{S_2}^* = \xi_{S_2} \sqrt{T_{CS_2}/T_{CS_1}}$ is the normalized coherence length in the S_2 layer, $\xi_{S_i} = (D_{S_i}/2\pi T_{CS_i})^{1/2}$. Here, the dimensionless parameters γ and γ_{BN} describe the nature of the interface between the two materials. They are defined by:

$$\gamma = \frac{\rho_{S_1} \xi_{S_1}}{\rho_{S_2} \xi_{S_2}^*}, \quad \gamma_{BN} = \frac{R_B}{\rho_{S_2} \xi_{S_2}^*}, \quad (5)$$

where ρ_{S_1} and ρ_{S_2} are the normal state resistivities and R_B is the product of the resistance of the S_1 – S_2 boundary and its

^{a)}Electronic mail: guy.brammertz@esa.int

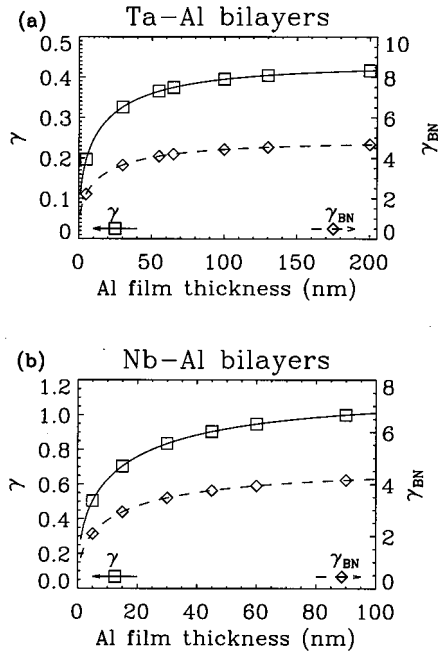


FIG. 1. Interface parameters γ (solid line, left-hand side scale) and γ_{BN} (dashed line, right-hand side scale) as a function of Al film thickness for (a) Ta-Al and (b) Nb-Al bilayers. Squares (γ , left-scale) and diamonds (γ_{BN} , right-hand side scale) indicate the points for which calculations of the energy gap and T_C were made.

area. Replacing the coherence length in the films by the dirty limit expression $\xi = \sqrt{\xi_0/3}$, where ξ_0 is the coherence length in the bulk material and l is the mean free path in the film, yields

$$\gamma = C_\gamma \sqrt{\frac{l_{S_2}}{l_{S_1}}},$$

with

$$C_\gamma = \frac{\rho_{S_1} l_{S_1}}{\rho_{S_2} l_{S_2}} \sqrt{\frac{\xi_{0S_1} T_{CS_1}}{\xi_{0S_2} T_{CS_2}}}, \quad (6)$$

$$\gamma_{BN} = C_{\gamma_{BN}} \sqrt{l_{S_2}},$$

with

$$C_{\gamma_{BN}} = \frac{R_B}{\rho_{S_2} l_{S_2}} \sqrt{\frac{3T_{CS_1}}{\xi_{0S_2} T_{CS_2}}}. \quad (7)$$

Here, the quantities C_γ and $C_{\gamma_{BN}}$ are independent of the thickness of the S_1 and S_2 films, because ρl is a material constant. The constant C_γ depends only on the nature of the two materials involved, whereas $C_{\gamma_{BN}}$ also depends on the quality of the interface between the two films. For bilayers deposited under similar conditions and having only different film thickness, the same values of C_γ and $C_{\gamma_{BN}}$ can be assumed. The dependence of the interface parameters on the film thickness can be determined by substituting the film thickness dependence of the mean free path into Eqs. (6) and (7). For complete electron scattering at the film surfaces, the following equation for the mean free path l as a function of film thickness d holds:²⁰

$$l = l_0 + l_0^2/d \left\{ \frac{3}{2} [E_3(d/l_0) - E_5(d/l_0)] - \frac{3}{8} \right\}, \quad (8)$$

where the exponential integrals are defined by $E_n(x) = \int_1^\infty t^{-n} e^{-xt} dt$ and l_0 is the mean free path in the bulk material.

Analytical solutions for T_C are possible only under certain limitations on layer thicknesses and interface parameters γ and γ_{BN} , as discussed earlier literature.⁷⁻¹⁸ In order to calculate T_C in the general case, we have solved the set of Eqs. (1) and (2) numerically. T_C is defined as the maximum temperature for which nontrivial solutions for the pair potentials Δ_{S_1} and Δ_{S_2} exist.

The devices studied in this work are symmetrical $S_1S_2IS_2S_1$ junctions, where every electrode is made out of a superconducting bilayer S_1S_2 . Two different kinds of devices are available, Ta-Al and Nb-Al based devices. The layers are deposited in an ultrahigh vacuum system. First a 100 nm thick layer of epitaxial Nb or Ta is laid down. Without breaking the vacuum, a polycrystalline Al film is then deposited on which a 10 Å Al-oxide barrier is grown. Then another polycrystalline Nb-Al or Ta-Al bilayer having the same film thickness as the base electrode is deposited on top of this oxide barrier. The thickness of the Al film depends on the sample and is varied between 5 and 200 nm. Details on material characteristics like bulk mean free path, residual resistance ratio, and bulk coherence length of the different films can be found in Ref. 21. All values given in the following are averages between the values for the top and base electrodes.

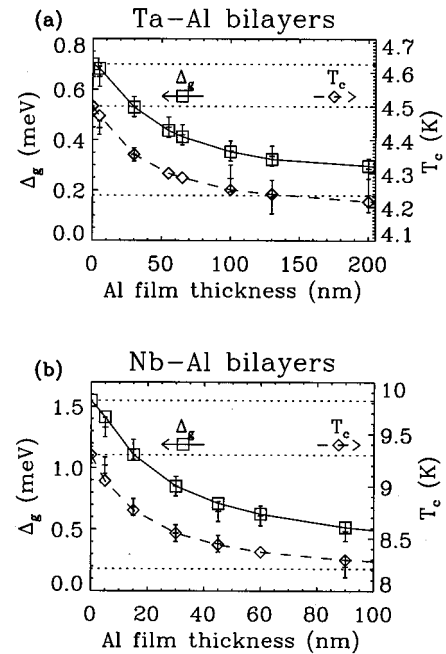


FIG. 2. Energy gap at 300 mK and T_C as a function of Al film thickness for (a) Ta-Al and (b) Nb-Al bilayers. The Ta and Nb film thickness has a constant value of 100 nm. Squares (Δ_g , left-hand side scale) and diamonds (T_C , right-hand side scale) represent the calculated values from our model. The solid (Δ_g , left-hand side scale) and dashed (T_C , right-hand side scale) lines are a guide for the eye between the calculated points. Crosses with error bars represent the corresponding experimental values. The dotted lines represent the bulk energy gap of Nb, Ta, Al, and the bulk T_C of Nb and Ta.

For every series of depositions (Ta or Nb based) the values of C_γ and $C_{\gamma_{BN}}$ are determined experimentally. The determination is based on a comparison between experimental and simulated values of the energy gap at 300 mK and the T_C of the bilayer. For the devices with 30 nm of Al from a deposition series, a number of simulations of the energy gap at 300 mK and the T_C with different values of γ and γ_{BN} are made. The model for the calculation of the energy gap of a superconducting bilayer is presented in Ref. 22. To a single pair of γ and γ_{BN} values corresponds a single pair of values of the gap at 300 mK and T_C .²¹ By applying Eqs. (6) and (7), the interface constants C_γ and $C_{\gamma_{BN}}$ can be determined. These were found to be equal to $C_\gamma=0.4806$, $C_{\gamma_{BN}}=0.6754 \text{ nm}^{-1/2}$ for the Ta–Al bilayers and $C_\gamma=1.372$, $C_{\gamma_{BN}}=0.642 \text{ nm}^{-1/2}$ for the Nb–Al bilayers. Knowing the values of C_γ and $C_{\gamma_{BN}}$ and using Eq. (8), we can now determine the interface parameters for the whole Al thickness range, leaving the Ta and Nb thickness constant at 100 nm. The results are shown in Fig. 1.

With the interface parameters from Fig. 1 as input parameters to our model, we can calculate the gap at 300 mK and the T_C of all different bilayers. The results of our simulations are shown in Fig. 2(a) for the Ta–Al bilayers and Fig. 2(b) for the Nb–Al bilayers. The agreement between theory and experiment is very good.

A model for the determination of the T_C of superconducting bilayers was presented. The model is valid in the dirty and in the clean limit with the condition of diffusive scattering at the film boundaries, with no restrictions to film thicknesses, T_C of the layers and resistivity of the superconductor–superconductor interface. Taking a layout of 100 nm of Ta or Nb topped with 30 nm of Al as a starting point in order to determine the interface parameters, we were able to predict the energy gap and the T_C of a whole range of

bilayers with different Al film thicknesses. The calculated values were compared to experimental values from Ta–Al and Nb–Al bilayers with Al film thicknesses ranging from 5 to 200 nm. The agreement between theory and experiment is very good for both the energy gap and the T_C .

- ¹P. A. J. de Korte, Nucl. Instrum. Methods Phys. Res. A **444**, 163 (2000).
- ²P. Verhoeve, Nucl. Instrum. Methods Phys. Res. A **444**, 435 (2000).
- ³N. Rando, A. Peacock, S. Andersson, B. Collaudin, P. Gondoin, J. Verveer, P. Verhoeve, D. J. Goldie, and R. Hart, Proc. SPIE **3435**, 74 (1998).
- ⁴C. A. Mears, S. E. Labov, M. Frank, M. A. Lindeman, L. J. Hiller, H. Netel, and A. T. Barfknecht, Nucl. Instrum. Methods Phys. Res. A **370**, 53 (1996).
- ⁵K. D. Irwin, G. C. Hilton, D. A. Wollman, and J. M. Martinis, Appl. Phys. Lett. **83**, 3987 (1998).
- ⁶K. A. Delin and A. W. Kleinsasser, Supercond. Sci. Technol. **9**, 227 (1996).
- ⁷P. de Gennes, Rev. Mod. Phys. **36**, 225 (1964).
- ⁸J. J. Hauser, H. G. Thenerer, and N. R. Werthamer, Phys. Rev. **136**, 637 (1964).
- ⁹W. Silwert and L. N. Cooper, Phys. Rev. **141**, 336 (1966).
- ¹⁰W. L. McMillan, Phys. Rev. **175**, 537 (1968).
- ¹¹B. Y. Jin and J. B. Ketterson, Adv. Phys. **38**, 189 (1989).
- ¹²K. D. Usadel, Phys. Rev. Lett. **25**, 507 (1970).
- ¹³A. A. Golubov, M. Y. Kupriyanov, V. F. Lukichev, and A. A. Orlikovskii, Mikroelektronika **12**, 355 (1983) [Sov. J. Microelectronics **12**, 191 (1984)].
- ¹⁴Z. Radovich, M. Ledvij, and L. Dobrosavljevic-Grujic, Phys. Rev. B **43**, 8613 (1991).
- ¹⁵A. A. Golubov, Proc. SPIE **362**, 353 (1994).
- ¹⁶M. G. Khusainov, JETP Lett. **53**, 579 (1991).
- ¹⁷Ya. V. Fominov and M. V. Feigelman, Phys. Rev. B **63**, 094518 (2001).
- ¹⁸J. M. Martinis, G. C. Hilton, K. D. Irwin, and D. A. Wollman, Nucl. Instrum. Methods Phys. Res. A **444**, 23 (2000).
- ¹⁹M. Y. Kupriyanov and V. F. Lukichev, Sov. Phys. JETP **67**, 1163 (1988).
- ²⁰D. Movshovitz and N. Wisner, Phys. Rev. B **41**, 10503 (1990).
- ²¹G. Brammertz, A. A. Golubov, A. Peacock, P. Verhoeve, D. J. Goldie, and R. Venn, Physica C **350**, 227 (2001).
- ²²G. Brammertz, A. Poelaert, A. A. Golubov, P. Verhoeve, A. Peacock, and H. Rogalla, J. Appl. Phys. **90**, 1, 355 (2001).